Design and biofabrication of a leaf-inspired vascularized cell-delivery device

Bioprinting 26 (2022) e00199

Contents lists available at ScienceDirect

Bioprinting

journal homepage: www.sciencedirect.com/journal/bioprinting

Design and biofabrication of a leaf-inspired vascularized cell-delivery device

Sanna Sämfors [a,1], Essi M. Niemi [b,c,d,e,1], Kristin Oskarsdotter [a], Claudia Villar Egea [a], Andreas Mark [f], Hanne Scholz [c,d,g], Paul Gatenholm [a,h,*]

[a] 3D Bioprinting Center, Wallenberg Wood Science Center, Department of Chemistry and Chemical Engineering, Chalmers University of Technology, Gothenburg, Sweden
[b] Department of Vascular Surgery, Oslo University Hospital, Oslo, Norway
[c] Institute for Surgical Research, Oslo University Hospital, Oslo, Norway
[d] Hybrid Technology Hub, Center of Excellence, Institute of Basic Medical Sciences, University of Oslo, Oslo, Norway
[e] Institute of Clinical Medicine, Faculty of Medicine, University of Oslo, Norway
[f] Fraunhofer-Chalmers Research Centre for Industrial Mathematics, Gothenburg, Sweden
[g] Department of Transplant Medicine, Oslo University Hospital, Oslo, Norway
[h] CELLHEAL AS, Sandvika, Norway

ARTICLE INFO

Keywords:
Biomimetic vascularized cell-delivery device
Mold casting
3D-bioprinting
Nanocellulose-alginate hydrogel
Endothelialization

ABSTRACT

We designed and biofabricated a channeled construct as a possible cell-delivery device that can be endothelialized to overcome size limitations due to oxygen diffusion. The channeled device mimicking a leaf was designed using computer-aided design software, with fluid flow through the channels visualized using simulation studies. The device was fabricated either by form casting using a custom 3D-printed plastic mold or by 3D-bioprinting using Pluronic F-127 as sacrificial ink to print the channels. The actual leaf was cast or bioprinted using hydrogel made from a mixture of tunicate cellulose nanofibers and alginate that was cross-linked in calcium chloride solution to allow a stable device. The resulting device was a 20 × 8 × 3 mm or 35 × 18 × 3 mm (length × width × height) leaf with one main channel connected to several side channels. Surface modification using periodate oxidation, followed by laminin bioconjugation, was performed to enhance endothelial cell adhesion in the channels. We subsequently used human umbilical vein endothelial cells to demonstrate the efficacy of the device for promoting endothelialization. These results indicated that the biofabricated device has great potential for use in tissue-engineering for various applications associated with the need of perfusable vasculature.

1. Introduction

Tissue engineering can potentially offer solutions to several problems in modern healthcare, including the shortage of transplantable organs. However, there has been little success in producing larger three-dimensional (3D) tissue structures. This can be attributed to the lack of vascularization in the developed structures and represents one of the largest hurdles in tissue engineering [1]. Without an established vascular system, engineered tissues rapidly lose viability due to the absence of systems capable of mass transport of nutrients, oxygen, and other factors, as well as removal of waste products. Successful fabrication of thick, vascularized, 3D tissues would represent a monumental achievement in regenerative medicine [2].

Fabrication of biomaterial-based scaffolds with an endothelialized vascular network *in vitro* is essential for supporting complex functional multicellular cultures and the creation of macroscale tissues that mimic the functionality of living tissues and organs. In tissues, the maximum distance of cells from the vasculature is ~200 μm, which highlights the need for efficient vascularization methods [1]. A biomaterial-based approach allows the specific creation of tissue-engineered constructs according to the material composition, vascular architecture, and dimensions necessary to support cell attachment, viability, angiogenic capacity, and function [3]. Building larger tissues and organs with vasculature systems and microvasculature with intricate hierarchy and resolution using current fabrication methods remains challenging [4]. Therefore, it is important to engineer biomaterials for vascular

* Corresponding author. 3D Bioprinting Center, Wallenberg Wood Science Center, Department of Chemistry and Chemical Engineering, Chalmers University of Technology, Gothenburg, Sweden.
E-mail address: paul.gatenholm@chalmers.se (P. Gatenholm).
[1] These authors contributed equally to this work.

https://doi.org/10.1016/j.bprint.2022.e00199
Received 26 November 2021; Received in revised form 20 January 2022; Accepted 14 February 2022
Available online 1 March 2022

approaches that can support efficient endothelialization and naturally stimulate angiogenesis between engineered vascular tissue and the surrounding matrix [5]. This type of vascularized and vascularization-promoting scaffold biomaterial would offer a versatile 3D-macroscale platform for the development of multicellular systems and devices that can combine the vascularized network with other cell and tissue types in order to create functional tissues and organs for *in vivo* analysis. Additionally, this type of scaffold could serve as a device for stem cell delivery [6–8], as well an artificial pancreas for the treatment of diabetes [9,10]. Several approaches have been evaluated for vascularizing tissue-engineered constructs, including adaptation of scaffold design to promote vascularization, incorporation of signaling molecules, such as growth factors, and fabrication of porous or channeled scaffolds [11–13].

A method used to incorporate channels into a scaffold involves use of a sacrificial template that leaves hollow structures after removal. This method has been used to create a simple vascular network on a chip that could potentially be used for the development of new vascular model systems [14]. Another study used carbohydrate glass as a sacrificial template along with an extracellular-matrix scaffold to create vascular architecture within a scaffold that was perfusable and maintained the function of embedded cells to a degree exceeding than of non-channeled scaffolds [15]. In our previous study, we used a 3D-printed vascular tree as a sacrificial template to produce a channeled network within a bacterial nanocellulose scaffold, revealing that the channels could be lined with endothelial cells as a first step toward vascularization and demonstrating the feasibility of 3D-printing for generating a sacrificial template for scaffold fabrication [16].

Another promising method for more precisely controlling scaffold architecture involves the use of 3D-bioprinting [5], where a 3D printer is adapted to print using various bioinks [17]. 3D-bioprinting has recently emerged as a tool for engineering vascular systems, as it allows for a controlled deposition of cells and other tissue constituents to create 3D constructs [18]. The use of bioink for these applications is a versatile method that shows potential for creating functional tissues that can be tailored to fit individual patients, which is an attractive prospect for applications related to personalized medicine. This method has been applied in several vascularization studies [19–21]. Additionally, Ouyang et al. [22] used 3D-bioprinting to print both matrix ink and template ink for layer-by-layer cell deposition, which allowed printing using bioinks previously considered difficult to print with due to structural collapse during the printing process. Moreover, they demonstrated that endothelial cells could be mixed with the templating bioink in order to allow lining of the inner surface of the channels with a confluent layer of cells [22].

Cellulose is the most abundant biopolymer in nature and has recently gained increased interest as a potential biomedical scaffold material [23]. A previous study demonstrated its biocompatibility [24], which is advantageous for its use as a scaffold. Additionally, studies report that stable 3D structures can be printed using nanocellulose mixed with alginate as a bioink [25]; however, cellulose exhibits poor cell-adhesive properties [26] that can hinder construct endothelialization. To address this limitation, cellulose can be chemically modified to enhance the cell-adhesive properties of the material through functionalization by formation of covalent bonds [27]. A previous study showed that 3D-printed nanocellulose–alginate hydrogels can be conjugated with protein to extend their functionality to new applications [28]. Moreover, sodium periodate oxidation of cellulose can be used to create dialdehyde cellulose, where the aldehyde groups can serve as anchors to support covalent binding of proteins [29]. Covalent attachment of collagen in cellulose sponges through sodium periodate oxidation is suitable for neural tissue engineering [30]. Furthermore, laminin bioconjugation is an attractive option for improving endothelial cell attachment to the nanocellulose–alginate hydrogel, as it is a major component of the healthy vascular wall basement membrane (BM), which is an essential cell-adherent extracellular-matrix layer that anchors the endothelial layer to the surrounding microenvironment [31,32]. The BM is comprised mainly of laminin isoforms 411 and 511 along with type IV collagen, heparan sulfate proteoglycan perlecan, the glycoprotein nidogen-1, and fibronectin [33]. Laminins interact with vascular endothelial cell receptors to assemble the protein network of the BM and function as initiators of the process in endothelial cells to produce and secrete type IV collagen that integrates the laminin network with perlecan and nidogens [33,34]. The synthesis and deposition of type IV collagen is essential for vascular cell adhesion and blood vessel formation, thereby highlighting the important role of laminin on vascular development and homeostasis [33].

The aim of this study is to show that we can design and biofabricate a biomimetic device, that in parts mimics the natural vasculature in a leaf. The biofabricated leaf-shaped device with hollow channels was surface modified to promote endothelialization. The aim was also to show that the leaf supports good viability of cells within the leaf device.

2. Materials and methods

2.1. Design and 3D-printing of the leaf mold

A leaf mold was created using computer-aided design (CAD) and comprised one leaf-shaped outer mold, four detachable side wings, and a middle rod. A small mold 20 × 8 × 3 mm (length × width × height) was printed by Acron Formservice AB (Anderstorp, Sweden). All parts were printed using a ProJet 7000 HD 3D printer (3D Systems, Cary, NC, USA) in Somos WaterShed 11122 photopolymer (DSM, Geleen, The Netherlands). A large mold 35 × 18 × 3 mm was printed using the 3D printer Form 2 (Formlabs, Somerville, MA, USA) in white resin (Formlabs).

2.2. Hydrogel preparation

Lyophilized sodium alginate powder (Pronova SLG100; NovaMatrix, Sandvika, Norway) was dissolved in sterile 4.6% D-mannitol aqueous solution (Sigma-Aldrich, Steinheim, Germany) until it formed a transparent alginate hydrogel (3%, w/v). Medical-grade tunicate nanocellulose hydrogel (2.5%; TUNICELL ETC; Ocean Tunicell AS, Blomsterdalen, Norway) was mixed by connecting two syringes with a luer lock adapter and transferring the solutions back and forth multiple times until creation of a homogeneous nanocellulose–alginate (80:20, vol%) composite hydrogel.

2.3. Fabrication methods of the leaf device

2.3.1. Casting of the leaf

3D-printed small leaf molds were sterilized by placement in ethanol, followed by transfer to Petri dishes to completely dry. The nanocellulose–alginate hydrogel was added to one side of the leaf mold, which was then flipped over, and another layer of nanocellulose–alginate hydrogel was then added to the other side. $CaCl_2$ cross-linking solution (100 mM) was added to cover the leaf devices, which were incubated overnight at 4°C. After cross-linking, the mold was removed by gently pulling out the side wings and the middle rod. The hydrogel leaves were then washed several times with Hank's buffered saline solution (HBSS; Sigma-Aldrich).

2.3.2. Fabrication of a leaf from human adipose tissue

Lipoaspirate from abdominal subcutaneous tissue was collected from a healthy female donor following approval from the Regional Ethics Committee of Gothenburg (Dnr 624-16) and receipt of written informed consent. Conventional water-jet-assisted techniques and Klein's standard tumescent solution were used. The lipoaspirate was processed with a Lipogems device (Lipogems International SpA, Milan, Italy) according to manufacturer instructions [35,36] using mechanical force and without any enzymatic treatment. Briefly, the lipoaspirate was washed

with a physiologic electrolyte solution (NaCl), emulsified by shaking with metal beads (4 times for 30 s), and rinsed in a closed system. After processing using the Lipogems device, the lipoaspirate was mixed with the nanocellulose–alginate hydrogel at a volumetric ratio of 1:4 (lipoaspirate:hydrogel). After thorough mixing, the resulting adipose–hydrogel was added to the large leaf mold by first applying hydrogel to one side, flipping it over, and applying another layer of adipose hydrogel. $CaCl_2$ solution (100 mM) was then added to cover the leaf. After cross-linking overnight, the mold was removed by gently pulling out the side wings and the main channel, and the adipose–leaf was washed several times with HBSS.

2.3.3. 3D-bioprinting the leaf

The CAD of the 3D-printed leaves was adapted for 3D-bioprinting of a leaf device using hydrogel bioink. The g-code was processed in Repetier–Host (Hot-World GmbH & Co. KG, Germany), and the leaf was scaled up to twice the original size in order to improve the resolution of the printed channels and ease overall handling. The leaf device was 3D-printed with the 3D bioprinter Inkredible (CELLINK AB, Gothenburg, Sweden) using dual-head printing and with the two printer heads loaded with nanocellulose–alginate bioink and Pluronic F-127 sacrificial ink (Sigma-Aldrich), respectively. After printing, the devices were crosslinked by applying 100 mM $CaCl_2$ solution and storage at room temperature overnight. The printed leaves were then placed on ice to ensure complete liquefaction of the sacrificial bioink. The liquid was aspirated by application of negative pressure by inserting a hypodermic needle into the main channel of the leaf. The empty channels were washed with cold deionized water to remove any residue, followed by a wash with the $CaCl_2$ crosslinking solution (100 mM) to make sure that the inside of the channels was crosslinked. The leaves were stored in HBSS for further experiments.

2.4. Surface modification of the leaf channels by laminin conjugation

Casted leaves were washed in HBSS, and excess liquid in the channels was removed using a pipette. The channels were oxidized by injecting 10 µl of 0.025 M sodium periodate solution in the main inlet and 10 µl in the main outlet using a small pipette, after which the devices were incubated at room temperature for 1 h in the dark. The oxidation solution was then removed, and devices were washed by injecting water in the inlet and outlet several times. Natural mouse laminin (Thermo Fisher Scientific, USA) was diluted in HBSS to a concentration of 100 µg/ml and injected (10 µl in the main inlet and 10 µl in the main outlet) with a small pipette, followed by incubation for 24 h at 37°C to allow bioconjugation. Excess protein solution was removed, and devices were washed by injecting HBSS several times.

2.5. In vitro cell studies on the leaf device

2.5.1. Leaf casted with adipose derived stem cells (ASC)

To investigate the ability to use the nanocellulose-alginate hydrogel together with cells in the material, the smaller leaf mold was used to cast the leaf with adipose derived stem cells (ASC). The cells were isolated, characterized and cultured as previously described [37] and approved by the Regional Committee for Medical and Health Research Ethics (REK 2017/976) for use in the experiments. Briefly, the cells were cultured to 80–90% confluence in complete medium; MEM alpha medium (Gibco, Thermo Fisher Scientific) containing 5% human plate lysate (HPL, Cook Medical, Bloomington, IN, USA) and 5 ug/ml Gentamicin (B. Braun Medical A/S, Frederiksberg, Denmark) before harvest using TrypLE Express (Gibco, Thermo Fisher Scientific). ASC count and viability (>95%) were determined using NC-200 (ChemoMetec, Allerod, Denmark). The experiments were conducted with cells in passage two.

12×10^6 cells ml^{-1} of ASCs were mixed carefully with the nanocellulose-alginate hydrogel, as previously described with two connected syringes back and forth approx. 50 times before casted into the small leaf mold. The ASC leaf devices were immediately crosslinked with $CaCl_2$ solution (100 mM) for 30 min and then washed with phosphate-buffered saline (PBS; Lonza Group AG, Basel, Switzerland) supplemented with 20 mM $CaCl_2$. The ASC leaf device was cultured in complete medium at 37°C and 5% CO_2 until cell viability assessment.

2.5.2. Endothelial cell seeding of the leaf device

Human umbilical vein endothelial cells (HUVECs; Lonza Group AG) were used for endothelialization studies of the leaf device. The cells were maintained and cultured in complete endothelial growth medium (EGM) supplemented with reagents from a SingleQuots kit (Lonza Group AG) at 37°C and 5% CO_2. HUVECs were cultured to 80–90% confluence before harvest using Trypsin/EDTA (Lonza Group AG). HUVEC count and viability (>95%) were determined using Countess II FL (Thermo Fisher Scientific). The experiments were conducted with cells at passage four.

To investigate how the surface modification affects the cell attachment and endothelialization potential of the nanocellulose-alginate hydrogel, HUVECs were seeded to small the leaf device on two consecutive days. This cell experiment included three sample groups: untreated nanocellulose–alginate leaves (Untreated Ctrl), leaves coated with laminin (100 µg ml^{-1}) for 24 h (C-Laminin), and oxidized leaves with bioconjugated laminin (OX/B-Laminin).

The devices were first washed by injecting PBS (Lonza Group AG) supplemented with 20 mM $CaCl_2$ into the main channel. The leaves then underwent three injections with 200 µl of EGM, transfer to a 12-well plate, and culture in 600 µl of medium for 30 min at 37°C and 5% CO_2. After incubation, the channels were washed again with fresh medium. Cell suspension (100 µl) was then slowly pipetted into the main channel of the leaf device at a cell density of 30×10^6 cells ml^{-1}, followed by addition of 1 ml medium to the wells and 30-min incubation at 37°C and 5% CO_2. At the end of 30 min, medium was added to a final volume of 2 ml, and at 2-h post-seeding, the leaf devices were flipped to secure even cell distribution and returned to incubation.

On day 1 post-seeding, the medium was removed, and the leaf devices were very slowly perfused with 200 µl of fresh medium. After this, the cell HUVEC seeding was repeated as it was done on day 0 of the experiment. Medium was changed daily during the experiment in order to provide continuous nutrients for the cells in the channels by first injecting 200 µl of fresh medium very slowly into the main channel and otherwise 3 ml to the wells. Samples were collected for live/dead analysis on days 4, 7 and 14, and also on day 4 samples were fixed with 4% paraformaldehyde (PFA, Santa Cruz Biotechnology, Dallas, TX, USA) supplemented with 20 mM $CaCl_2$ for 20 min for further analysis.

2.6. Cell viability assessment of the leaf devices

Cell viability of the leaf devices was assessed by fluorescein diacetate (FDA; Sigma-Aldrich) and propidium iodide (PI; Thermo Fisher Scientific) staining. Samples were collected from the ASC leaf on day 1 and the HUVEC leaf on days 4, 7 and 14 post-seeding. ASC leaves were stained as whole device, whereas HUVEC leaf devices were first cut open using a microtome blade to reveal the channel network. Samples were incubated with FDA (20 µg ml^{-1}) and (PI (100 µg ml^{-1}) in PBS supplemented with 20 mM $CaCl_2$ for 5 min in the dark. Viable cells are stained green (FDA), and dead cells are stained red (PI). The samples were imaged under an Axio Observer inverted microscope (Carl Zeiss AS, Oberkochen, Germany) and Zeiss ZEN Blue software using z-stacks with 12–15 µm steps depending on the shapes of the surfaces to ensure sufficient imaging of the 3D structure.

2.7. In vivo evaluation of the surface modified hydrogel

To assess *in vivo* the surface modified hydrogel with HUVECs, simplified half-channeled circular hydrogel scaffolds were prepared for subcutaneous implantation with same groups as in the endothelialization experiments: Untreated Ctrl, C-Laminin, OX/B-Laminin and in

addition, untreated cell free circular scaffolds (Cell-free Ctrl) served as a negative control. To prepare the scaffolds, 1 mm thick layer of the nanocellulose-alginate hydrogel was dispensed to a Petri dish and sterile acupuncture needles (250 μm diameter) were placed parallel on the hydrogel surface by gently pressing them into the layer with help of tweezers. The layer was crosslinked with sterile $CaCl_2$ (100 mM) solution for 30 min in RT. The needles were removed after crosslinking from the hydrogel resulting in half-cylindrical indentures or "half-channels" with a radius of ~125 μm. An 8 mm sterile biopsy punch tool was used to create circular half-channeled scaffolds. The scaffolds were washed with sterile $CaCl_2$ (100 mM). The oxidation and laminin bioconjugation were performed as described in **2.4**.

The circular half-channeled scaffolds were cultured on a 48 well plate, 300 μl of EGM medium was added and incubated for 30 min at 37°C. Medium was removed and cell suspension (100 μl) of HUVECs was added on the scaffolds with 9×10^5 cells cm^{-1} density. The scaffolds were returned to the incubator and 500 μl of EGM was added after 2h of incubation. The scaffolds were kept in culture, and medium was changed daily. On day 4 of culture post-seeding, scaffolds were transplanted subcutaneously to the side of Rag1 KO mice in triplicates, channeled side facing inwards. The transplantation site was closed with surgical clips. The mice were observed daily and weighed every seven days by an animal technician. The scaffolds were harvested on day 33 post-transplantation and fixed with 4% PFA, washed three times 10 min and stored to PBS, both reagents supplemented with 20 mM $CaCl_2$ for further analysis.

2.8. Immunohistological analyses of the biomaterial devices

Retrieved circular hydrogel scaffolds were prepared for cryosectioning by incubating the scaffolds in solutions of 15% and 30% sucrose (Sigma Aldrich) in PBS, followed by 30% sucrose - Tissue-Tek OCT (Sakura Finetek Norway AS, Oslo, Norway) compound (1:1 v/v ratio), all steps o/n at 4 °C and all solution supplemented with 20 mM $CaCl_2$. Finally, the samples were embedded to OCT, half channels orthogonally positioned towards the cutting surface, frozen with liquid nitrogen, stored to −20°C before serially sectioned of 20 μm sections using CryoStar NX70 (Thermo Fisher Scientific).

The samples were first permeabilized with 0.3% Triton-X100 (Sigma-Aldrich) in PBS for 15 min (30 min) and then incubated 1.5% donkey serum (Millipore, Burlington, MA, USA) in PBS for 1h to block nonspecific sites. The following primary antibodies were used diluted to PBS: sheep polyclonal human specific CD31 (5 μg/mL; hCD31; R&D Systems Norway, Abingdon, UK), goat polyclonal mouse specific CD31 (5 μg/mL; mCD31; R&D Systems Norway), rat monoclonal CD34 (1:200; Thermo Fisher Scientific) and rabbit polyclonal VE-Cadherin (1:300; Abcam, Cambridge, UK), incubated overnight (2 days) at 4°C. Afterwards, samples were washed three times in PBS and incubated 2 h at RT (overnight at 4°C) with secondary antibodies diluted to 1.5% donkey serum in PBS: donkey anti-rabbit AlexaFluor488 (1:800), donkey anti-sheep AlexaFluor488 (1:800), donkey anti-rat AlexaFluor594 (1:800) and donkey anti-goat AlexaFluor594 (1:800), followed by three washes with PBS (10 min/wash) supplemented only with 10 mM $CaCl_2$. Nuclear staining for the cryosectioned samples was performed with hardening VECTASHIELD® Vibrance™ Antifade Mounting Medium with 4′,6-diamidino-2-phenylindole (DAPI; Vector Laboratories, Burlingame, CA, USA) and the opened *in vitro* endothelialized leaf device samples with Invitrogen SlowFade Gold Antifade Mountant with DAPI (Thermo Fisher Scientific). The incubation steps presented in brackets are for the cut open *in vitro* endotheliazation samples to ensure proper staining. All staining steps were performed at room temperature unless otherwise stated, and all reagents were supplemented with 20 mM $CaCl_2$ to ensure the integrity of the hydrogel material. All the prepared samples were imaged with an Axio Observer inverted microscope and analyzed with Zeiss ZEN Blue software. The cut open samples were imaged as z-stack similarly as explained in 2.6.

2.9. Flow simulation

To evaluate the flow inside the leaves, we used a computational fluid dynamics simulation tool (IPS IBOFlow) [38]. The simulation tool was developed at Fraunhofer–Chalmers Research Centre and efficiently handles complex geometries using a unique immersed-boundary method [39]. The inputs to the solver are the thermodynamic properties of the fluid and a triangulation of the geometry (leaves), that are assumed to be rigid. In the simulation, the inlet velocity is established, and the resulting flow and fluid forces are calculated and visualized in ParaView [40]. The inlet velocity was chosen based on an approximation of the volume flow rate of blood inside the arteries of a human finger [41].

3. Results and discussion

3.1. Biomimetic design of the device

Human vasculature is comprised of a hierarchical and complex structure, A more simplistic vascular structure can be found in nature in the form of leaves (Fig. 1). The veins in a leaf resemble the capillary beds sprouting from larger vessels similar to those found in the human body; therefore, a leaf can be considered an excellent model on which to base the design of a vascular network. The venation pattern in leaves varies between species (Fig. 1A); however, the primary purpose of venation in all species is to provide water and nutrients to all regions. Pinnate venation is a simpler pattern that comprises one main channel with multiple branched side channels (Fig. 1B). This is an intriguing model, as it fulfills the requirement that the network reach all parts of the device, as well as remaining simple enough for fabrication and reproducibility. In this study, we based the mold design on the pinnate venation structure, where one main channel with an inlet and outlet is connected to several branched side channels. The model was adapted to fit the concept of self-vascularization by extending the side channels to the edge of the device, thereby providing multiple inlets for capillaries to grow into when placed *in vivo*.

3.2. Design and 3D-printing of a leaf mold for casting with cells

The biomimetic mold was 3D printed using either white resin or Somos WaterShed 11122 photopolymer. Both materials provided satisfactory results, with good resolution capable of acquisition for all printed parts. The designed mold comprised an outer form in the shape of a leaf with cut-out holes for insertion of the rod to create the main channel and the side wings to create the branched channels on both sides of the main channel (Fig. 2A and B).

The mold can be 3D printed in any size depending on the application. However, there is a size limitation especially when it comes to making small sizes that is depended on the resolution of the 3D printer used for printing the leaf mold. In this study, we fabricated two different sizes: a large one that was easily assembled as a proof-of-concept and a smaller one ideal for *in vivo* mouse studies (Fig. 2C). The larger mold created a device with dimensions of 35 × 18 × 3 mm (length × width × height), and the smaller mold had dimensions of 20 × 8 × 3 mm. In both cases, the molds were easy to assemble and disassemble, which is important for reuse of the same mold multiple times.

The mold was then used to produce a hydrogel leaf by casting the nanocellulose–alginate hydrogel (Fig. 2D), after which the mold was covered in $CaCl_2$ solution in order to cross-link the alginate and form a stable leaf device. After cross-linking, the inserts were easily removed, creating hollow channels in the casted device resembling the structure of leaf veins (Fig. 2E). This cast design was highly reproducible, as each casted leaf will be identical when using the mold. Upon visual inspection the channel geometry and size were similar to the mold and no collapsing of the channels were observed in any of the casted leaves nor swelling of the channels. To ensure that all side channels were connected

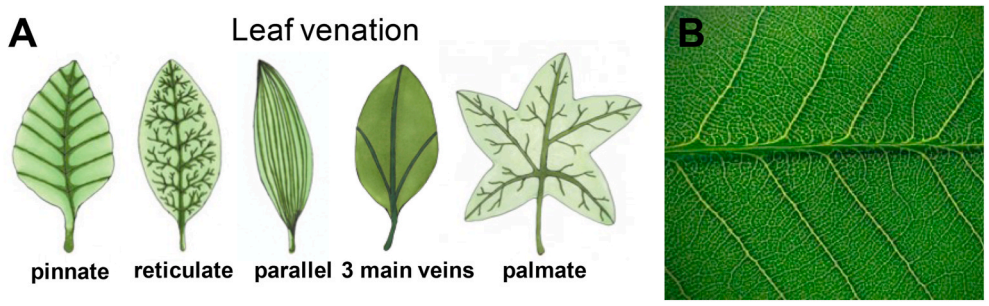

Fig. 1. Vascularization in nature used as inspiration of the proposed biomimetic device. (A) Various examples of leaf venation existing in nature. (B) Close-up view of pinnate leaf venation comprising a main channel branching to multiple side channels that allow nutrients to reach all parts of the leaf (image adapted from Pixabay, Germany).

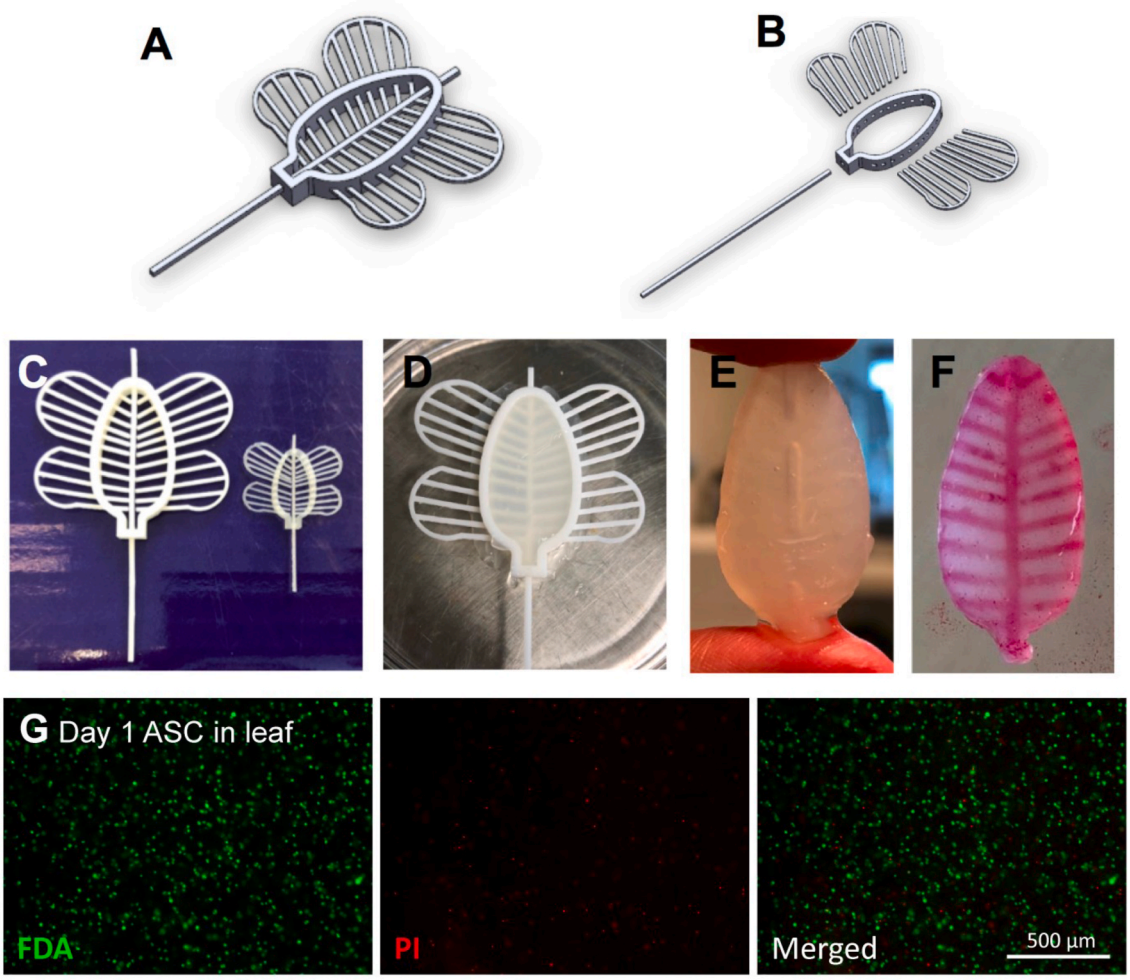

Fig. 2. Fabrication of a mold for casting a leaf and viability of adipose derived stem cells (ASC). A CAD model inspired from a leaf with one main channel and four removable wings. (A) The assembled form of the mold, and (B) the removable parts of the design. The mold can be made in various sizes depending on use. (C) Examples of two different sizes. (D) Cellulose hydrogel added to the mold for leaf casting. (E) Cast leaf after cross-linking and removal of the mold. (F) Leaf channels perfused with water colored with a few drops of red food dye for visualization. Viability of the ASCs in the leaf device (G) at day 1. Scalebar 500 µm. (For interpretation of the references to color in this figure legend, the reader is referred to the Web version of this article.)

to the main channel, the inlet of the main channel was injected with colored water, after which we confirmed that the colored water had been dispersed in all of the branched channels, proving that the fluid could easily reach all parts of the leaf (Fig. 2F) and confirming that no channel collapse had occurred.

To assess usability of the device for cell delivery, cell viability inside the leaf device, adipose derived stem cells (ASC) were mixed with the nanocellulose-alginate hydrogel and casted using the small leaf mold. Cell viability was determined by performing a live/dead stain one day after casting and four days after casting. At day 1, the majority of the ASCs inside the leaf (Fig. 2G), was stained in green indicating that there were many living cells and the cells withstood well the casting process of the leaf. A few dead cells could also be located inside.

3.3. Leaf made with human adipose tissue

As a proof-of-concept experiment to demonstrate leaf fabrication using various hydrogels depending on the application, we used the larger leaf mold to make a leaf using human adipose tissue. The tissue was taken from a liposuction procedure, where the resulting lipoaspirate was processed using mechanical forces to break down the tissue into a homogenous dispersion, using a Lipogems device designed for gently harvesting and processing of fat tissue [35,36]. The homogenized tissue was mixed with nanocellulose–alginate hydrogel to form an adipose–hydrogel. The addition of nanocellulose provides modification of the rheological properties for easy extrusion, whereas the alginate offers the ability of the hydrogel to be cross-linkable using divalent cations [42]. The hydrogel was easily applied to both sides of the leaf mold (Fig. 3A), and the leaf could be cross-linked using $CaCl_2$ solution to form a stable 3D device with internal channels (Fig. 3B and C). The mold was easily removed by slowly pulling out the side wings and middle rod, leaving intact channels. The fabricated leaf was robust and could be stored in HBSS for several days without disintegrating. These results indicated that the leaf mold could be used for fabrication of various tissue devices depending on the biomaterial used. Both the nanocellulose–alginate hydrogel and adipose tissue were successfully cast onto the leaf mold, which after cross-linking formed a stable 3D device.

3.4. 3D-bioprinting of a leaf using hydrogel ink

The mold-casting process allowed production of reproducible hydrogel or adipose leaves; however, the process can be made more efficient and automated by the use of 3D-bioprinting technology. Therefore, based on the mold design, we developed a g-code (Fig. 4A) that could be used to fabricate a leaf by 3D-bioprinting using dual-head printing with both structural and sacrificial bioink (Fig. 4B). We printed a leaf using a structural bioink (nanocellulose–alginate hydrogel) for the body and a sacrificial ink (Pluronic F-127) for the channels. Due to the thermo-reversible nature of Pluronic F-127, the channels could be evacuated after cross-linking by cooling the leaf (Fig. 4C), which transformed Pluronic F-127 into a fluid with low viscosity and ultimately left hollow channels inside the device. The resulting prototype (or device) was robust and easy to handle, and the sacrificial material was evacuated after cooling. No signs of channel collapse or channel swelling could be detected. To visualize perfusability, the device was perfused with water mixed with food dye using a syringe and hypodermic needle (Fig. 4C). The leaf was easily perfused in this manner and showed no noticeable leakage. The channels were clearly connected and formed an interconnected network within the device. Additionally, the device was compatible with a perfusion system that uses a peristaltic pump, making it an interesting target for further use in cell studies where circulation of cell medium would provide a more natural environment for cells, such as endothelial cells.

The results obtained using these 3D bioprinted models demonstrated the feasibility and versatility of 3D-bioprinting for fabrication of perfusable devices with a high degree of accuracy. 3D-bioprinting allows production of different vascular models of increasing complexity, which after combination with a perfusion system can potentially provide a suitable physical environment for endothelial cells. The device could also be printed in any size, depending on the application, where the size limitation for how small leaf you can print is dependent on the printing resolution of the bioprinter used.

3.5. Surface modification and endothelialization of the device

Since it was shown preserved viability of the ASC leaf, we wanted to investigate the possibility to endothelialise the inside of the channels within the leaf. The channels of the small leaf device made from nanocellulose-alginate hydrogel by casting were seeded with HUVECs, and the medium was changed daily to ensure a constant flow of sufficient nutrients to cells in the channel network. Additionally, we assessed static culture without perfusion with medium and injecting medium with a pipette as culture options. We found that static culture affected cell viability in the channels due to restricted flow, which resulted in increased cell death.

Medium was injected extremely slowly to the main inlet to avoid disturbing cell attachment and proliferation in the channel network. Previous studies have demonstrated the importance of slow perfusion of medium for effective endothelialization [22,43]. Future work should evaluate the effectiveness of connecting the leaf to a perfusion system to mimic the shear stress encountered in blood vessels in order to improve potential endothelialization. Vascular endothelial cell function is heavily affected by the hemodynamic forces of blood flow, which directs vascular development, vascular endothelial cell morphology, phenotype, and overall cell behavior [44].

Nanocellulose scaffolds have previously been shown to have low cell attachment [26]. In order to increase the cell attachment to the nanocellulose-alginate hydrogel channels, the channel surfaces were

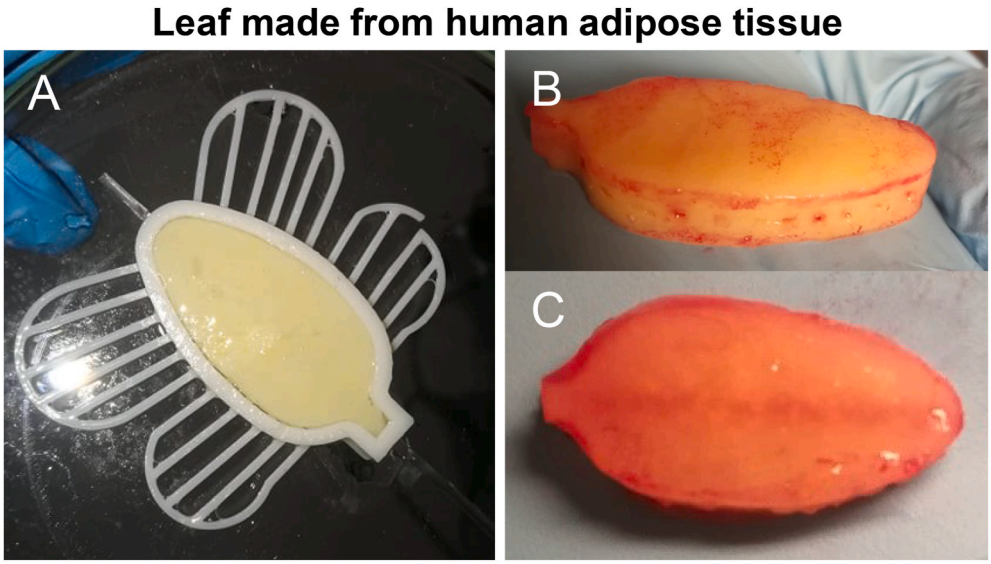

Fig. 3. Leaf made from human adipose tissue (A) Adipose nanocellulose–alginate casted inside a leaf mold. Side view (B) and top view (C) of an adipose leaf after cross-linking and mold removal.

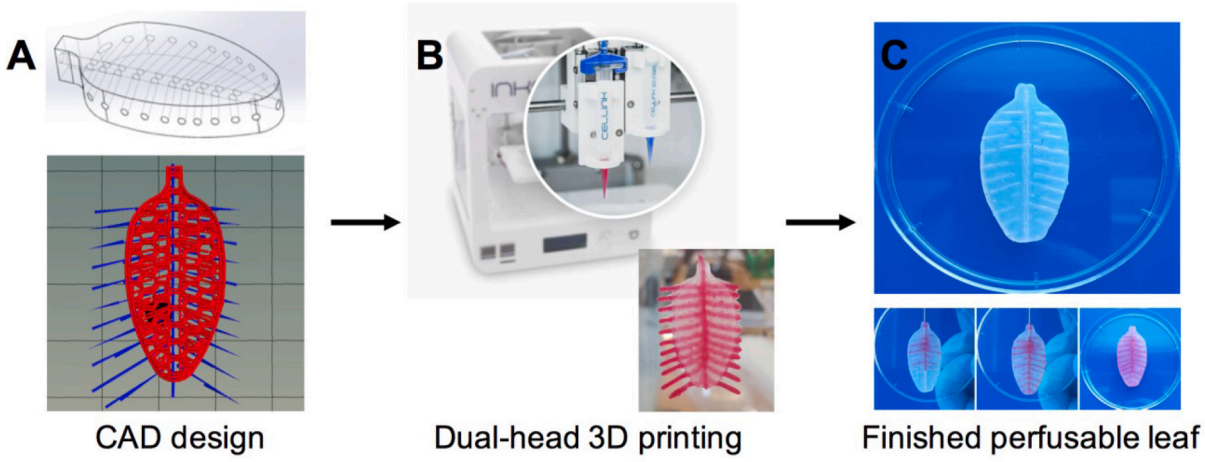

Fig. 4. Leaf fabrication using 3D-bioprinting technology. A CAD was created using the mold for casting. (A) The final design of the leaf, with the bulk of the leaf in red, and channels shown in blue. (B) A dual-head 3D bioprinter used to print the bulk of the leaf using nanocellulose–alginate ink and sacrificial ink (Pluronic F-127) for the channels (red). (C) A finished leaf with the sacrificial ink removed. The leaf was perfusable with water colored using a few drops of red food dye for visualization (pictures at the bottom). (For interpretation of the references to color in this figure legend, the reader is referred to the Web version of this article.)

treated using oxidation and laminin bioconjugation. The treatment was assessed by comparing viability and attachment of endothelial cells inside the channels between untreated leaves (Untreated Ctrl), leaves with laminin coating (C-Laminin) and surface treated leaves with oxidation and laminin (OX/B-Laminin). Viability assessment in the channel networks was performed on days 4, 7 and 14 post-seeding with live/dead staining.

On day 4 post-seeding (Fig. 5), all groups showed HUVEC attachment to the walls and areas of endothelial lining in the network channels. Untreated Ctrl samples showed lower viability and only local attachment of cells in the channels whereas C-Laminin samples showed more endothelialized areas, but less tubular-network formation compared to the OX/B-Laminin samples. OX-B-Laminin samples showed to have most endothelial layer-like areas to cover channel walls on day 4 (Fig. 5A). Similar trend continued to day 7 (Figs. 5B) and 14 (Fig. 5C), as the Untreated Ctrl samples showed a low number of cells and only minimal and local areas with cells on the channel walls. On day 7, C-Laminin and OX/B-Laminin samples showed clear cell linings on the channel walls and more endothelialized areas, but C-Laminin showed lower cell viability and some clumps of dead cells. By day 14, the C-laminin samples showed to have lower cell viability whereas the OX/B-laminin showed very good cell viability and cell coverage in larger areas in the channel network.

Additionally, the leaf devices underwent immunofluorescence staining on day 4 post-seeding for the endothelial cell marker CD31, the tight junction marker VE-Cadherin, BM protein laminin and endothelial progenitor cell marker CD34 to visualize endothelialization and communication of the attached HUVECs in the channel network of the leaf device.

These results agreed with those from live/dead cell staining on day 4, C-Laminin and especially OX/B-Laminin samples showed (Fig. 6A) evidence of better endothelialization, cell junctions and increased viability as compared with Untreated Ctrl samples. hCD31 was expressed all of the groups, but clearer in both of the laminin groups, to show intercellular tight junctions for paracellular exchange of ions and solutes between confluent cells [45,46] the transmembrane protein vascular endothelial, VE-Cadherin, was only slightly expressed for adherens junctions in all of the groups. It is an important parameter for contact integrity and adhesive interactions between endothelial cells [47]. The absence of stronger and more organized indication of VE-cadherin could be due the lack of flow in the culture conditions as it has been shown that interactions between endothelial cells increase via VE-cadherin in the presence of flow through mechanotransduction [48].

The results showed that laminin (Fig. 6B) was expressed in the laminin groups slightly more compared to the Untreated Ctrl. This supports the results that the use of laminin, either by coating bioconjugation has aided the endothelialization process compared to the untreated sample and could indicate that the present endothelial cells to have started to produce their own laminin. CD34 was stained to observe if the cells would have expressed vascular endothelial progenitor cell phenotypic properties for angiogenesis and it was slightly expressed in the laminin groups compared to the Untreated Ctrl. It could too early on day 4 for the HUVECs to acquire such phenotype and also, CD34 is mostly observed in small and newly formed vessels [49] whereas the channel network in the leaf device simulates larger blood vessels than capillaries.

Overall, these results from live/dead and immunofluorescent staining emphasized the importance of biomaterial surface modification and immobilization of proteins by bioconjugation to the surface of the nanocellulose–alginate hydrogels to allow longer-term cell attachment and endothelialization potential.

3.6. *In vivo evaluation of the oxidized nanocellulose-alginate hydrogel*

To study the oxidized nanocellulose-alginate hydrogel combined with bioconjugated laminin *in vivo*, the leaf device design was simplified to an open half-channeled circular disc model, surface treated and seeded with HUVECs. The circular scaffolds were transplanted subcutaneously four days post-seeding to Rag1 KO mice and harvested on day 33 post-transplantation (Fig. 7). In all experimental groups, the scaffolds had attached to the surrounding tissue, and especially tightly in the OX/B-Laminin group. Some thin vascularization was visible around some of the scaffolds. All the scaffold had seemed to keep their shape well throughout the experiment, except a Cell-free Ctrl scaffold had broken down slightly and lost its round shape.

The harvested scaffolds were cryosectioned to observe the cross-sections of the circular disc scaffolds. The samples were embedded in OCT the way that the open half channels were positioned orthogonally to the cutting surface but the surrounding tissue upon harvest made positioning the scaffolds correctly quite challenging. This way it was possible to stain and observe the cells in the half-channels. The sections were stained with hCD31 and mCD31 to study the cells on the surfaces of the scaffolds, if they were the seeded HUVECs and/or cells from the mouse. hCD31 was not visible in the samples which would indicate that the HUVECs were not present at day 33 post-transplantation, and DAPI indicates presence of mouse nuclei in the samples rather than human

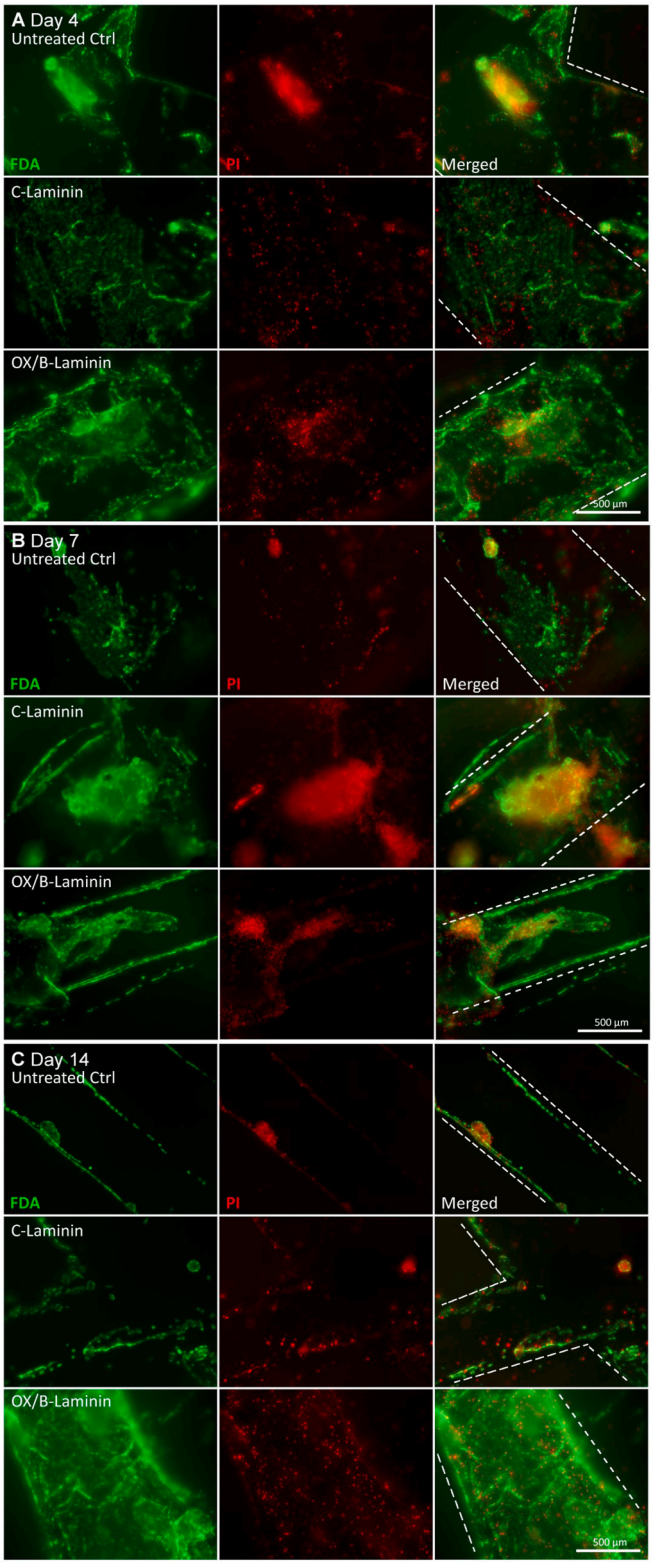

Fig. 5. Live/dead cell staining of the endothelialized leaf devices with FDA/PI. Samples were imaged on days 4 (A), 7 (B) and 14 (C) to evaluate endothelialization and cell viability in the different experimental groups. Untreated Ctrl, untreated nanocellulose–alginate leaf devices; C-Laminin, leaf devices with only a laminin coating; and OX/B-Laminin, oxidized leaf devices with bioconjugated laminin. Scalebar: 500 µm. Lines have been added to indicate where the channels are located inside the leaf device.

cells. In addition, we could observe some mCD31 positive staining co-localized with DAPI, however, we might also have some unspecific mCD31 in these samples. Overall, all groups, Untreated Ctrl, C-Laminin, OX/B-Laminin and Cell-free Crtl showed similar results. It seemed that host animal cells grew well on the surfaces on the transplanted biomaterial and also if there were openings in the material, the cells seemed to grow into the material, but no other ingrowth was observed.

3.7. *Flow simulations*

To assess the possibility of connecting the leaf to a perfusion bioreactor, the leaf design was evaluated with water at room temperature and with respect to the flow parameters inside the channels. Wall shear stress is a parameter used to evaluate forces parallel to the vessel wall and assess how flow might affect cell attachment to the wall. To understand the parameters influencing flow, we investigated three different channel geometries. The first was the same design used for printing the 3D mold that consisted of straight channels with one inlet and one outlet and where the side channels were considered to be closed at the ends. The second geometry consisted of cone-shaped side channels, and the third geometry involved the design using the cone-shaped side channels but with no open geometries (the ends of the channels were connected to the inlet and outlet). Fig. 8 shows the simulated wall shear stress and flow field for each of the leaf designs. The relatively high Reynold's number and momentum-dominated flow indicated that the highest velocities occurred in the central channel. Additionally, the large angle of the lateral channels resulted in unwanted recirculating regions and creeping flow; therefore, the geometric configuration was not optimal. Future simulations should apply geometrical optimization to minimize recirculation in the identified regions and improve flow in the lateral channels. Interestingly, the wall shear stress did not appear to be affected by recirculation and the flow-separation area, given that it increased along with the flow velocity. However, this does not suggest an absence of risk for developing arteriosclerosis, given that this is a condition that appears when endothelial cells are exposed to uneven wall shear stress over extended periods of time.

3.8. *Future perspectives*

In the various experiments that have been included in this paper, we show the versatile nature of the designed biomimetic leaf device. The device can be fabricated in different sizes with different fabrication methods and the flexibility opens up for the possibility to be used in different application areas. We show that cells can stay viable in the leaf for up to 14 days, however this time period is likely to be extended by the use of a perfusion bioreactor. This allows for the use in e.g. drug screening studies where cell response to different drugs can be better assessed due to more natural culturing conditions inside the 3D leaf. It also provides a platform to study co-cultures of endothelial cells and other cell types by having endothelial cells attach in the channels and mixing other cell types in the bulk of the hydrogel-alginate leaf. The ability to maintain viable cells within the leaf also opens up for the ability to be used as a cell delivery device *in vivo*. To be able to become a successful cell delivery device it needs to be able to support viability of cells within the material as well as allow for the ability to vascularize the device. When placed *in vivo* the device needs to be connected to the existing vascular systems and support endothelialization by allowing endothelial cell attachment, something we show is possible by using chemical modification inside the channels. As an example, the device could be used for delivering insulin producing islets of Langerhans for the treatment of diabetes. The islets would be placed inside the leaf and the channels would allow for nutrients to reach all parts of the device as well as simplifying the secretion of insulin to the surrounding tissue.

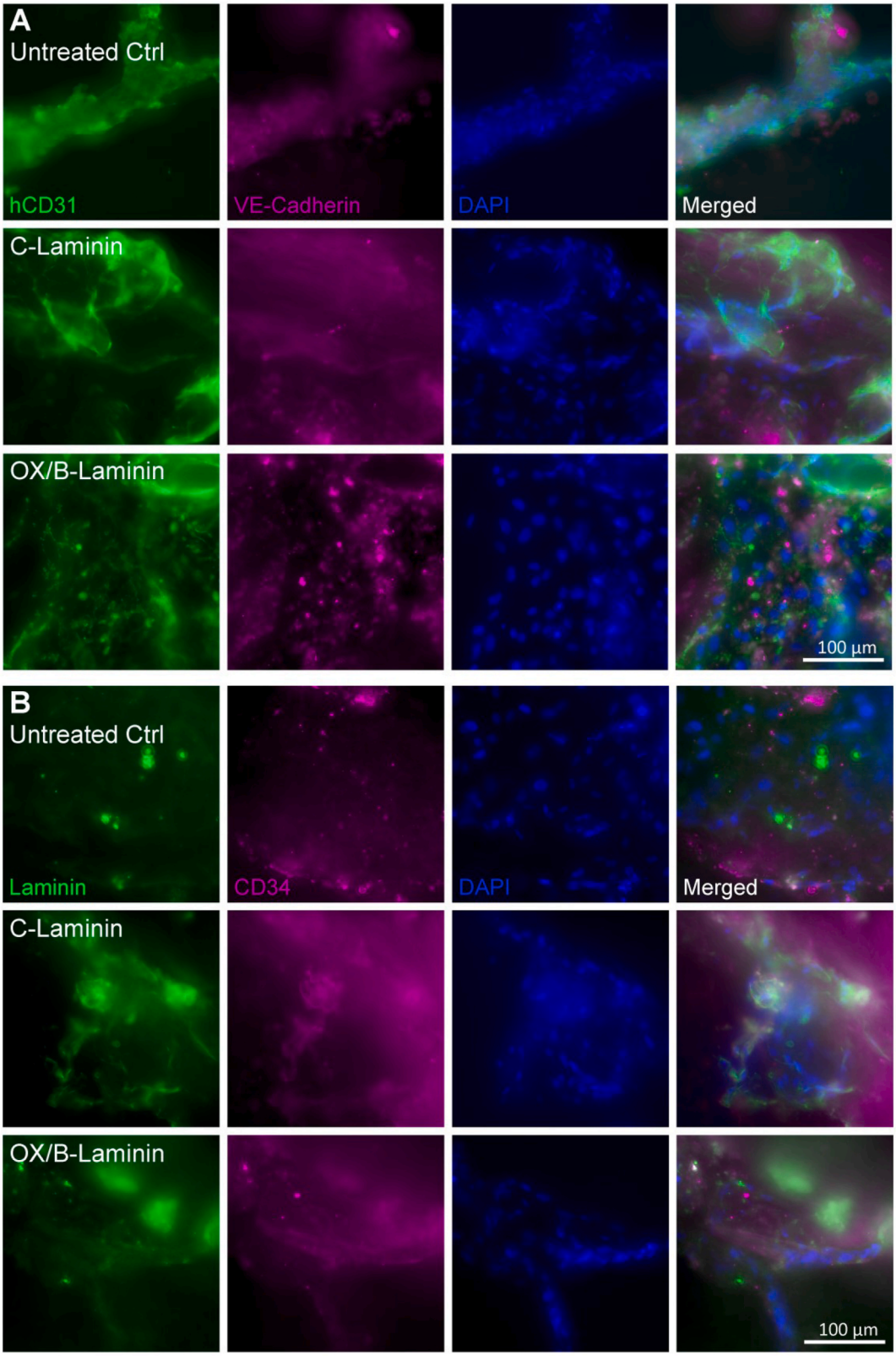

Fig. 6. Immunofluorescence staining of the endothelialized leaf devices. Staining was performed on day 4 post-seeding. Staining targeted the endothelial cell marker A) hCD31, the tight junction marker VE-Cadherin (VE-Cad) and B) BM protein laminin and endothelial progenitor cell marker CD34. Untreated Ctrl, untreated nanocellulose–alginate leaf devices; C-Laminin, leaf devices with only a laminin coating; and OX/B-Laminin, oxidized leaf devices with bioconjugated laminin. Scalebar: 100 µm.

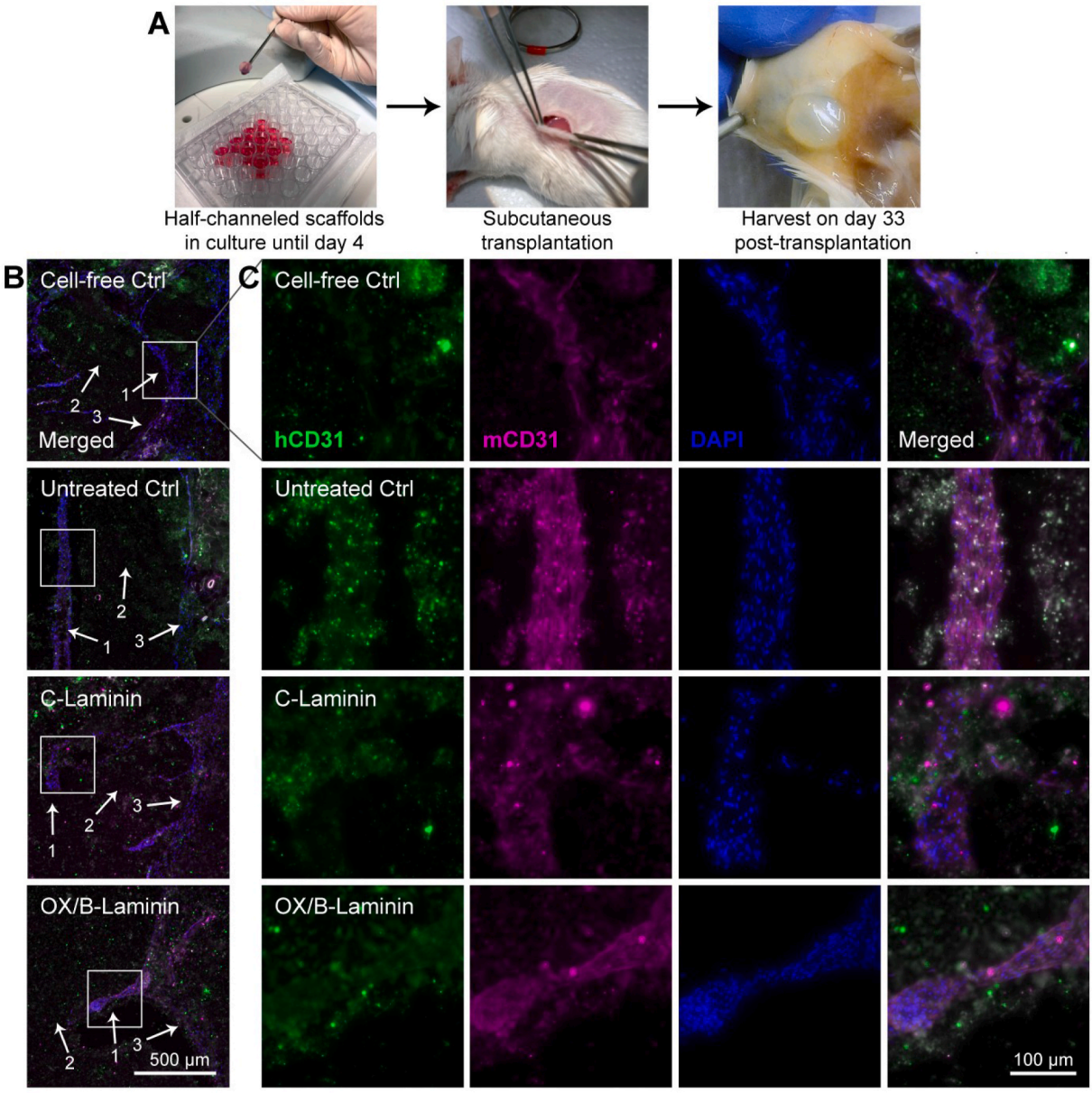

Fig. 7. Subcutaneous transplantation, harvest and immunofluorescent staining of the half-channeled circular scaffolds. A) Half-channeled scaffolds were cultured until day 4 with HUVECs, followed by subcutaneous transplantation to Rag1 KO mice and harvested on day 33 post-transplantation. Staining targeted hCD31 and mCD31 on 20 µm frozen cross-sections. B) Greater areas shown from the scaffolds to identify 1) cells inside the biomaterial, 2) the biomaterial and 3) surrounding tissue from the animal. Scalebar 500 µm. Squares indicate in C) areas shown for more detailed staining results. Scalebar 100 µm.

4. Conclusion

In this study, we described the design and biofabrication of a leaf-inspired device that can be fabricated using two different techniques. The device can be made using both a 3D-printed mold that can be easily removed after casting using different hydrogels or by 3D-bioprinting of the entire device using a combination of bioink and sacrificial ink. Both methods allowed fabrication of a robust 3D device with interconnected and perfusable channels. The casting method offers a rapid, highly reproducible, and simple fabrication method, whereas the 3D-bioprinting method allows for a greater ability to control and easily change the leaf design. As a proof of concept, we showed that the leaf could be made using by adding adipose tissue or adipose derived stem cells inside the hydrogel before casting. Furthermore, the inside surface of the channels can be chemically modified using sodium periodate oxidation, followed by bioconjugation with laminin in order to improve endothelial cell attachment. The results demonstrated that endothelial cells remained viable inside of the laminin-bioconjugated channels for up to 4 days, as these surfaces promoted HUVEC attachment and endothelialization. The treated surfaces were also shown to be biocompatible *in vivo* Furthermore, flow simulations in the channels suggested the possibility of geometrical optimization to provide an optimal design to allow for laminar flow inside the channels, which would support device connection to a bioreactor for expanded assessment of endothelialization potential. This design has potential as device to promote safe delivery of cells *in vivo* while simultaneously supporting their sustained viability through endothelialization. These results suggest the proposed device as a first step towards the creation of larger tissue devices for *in vivo* use, as well as application as a perfusion bioreactor allowing *in vitro* study of organ development and drug screening.

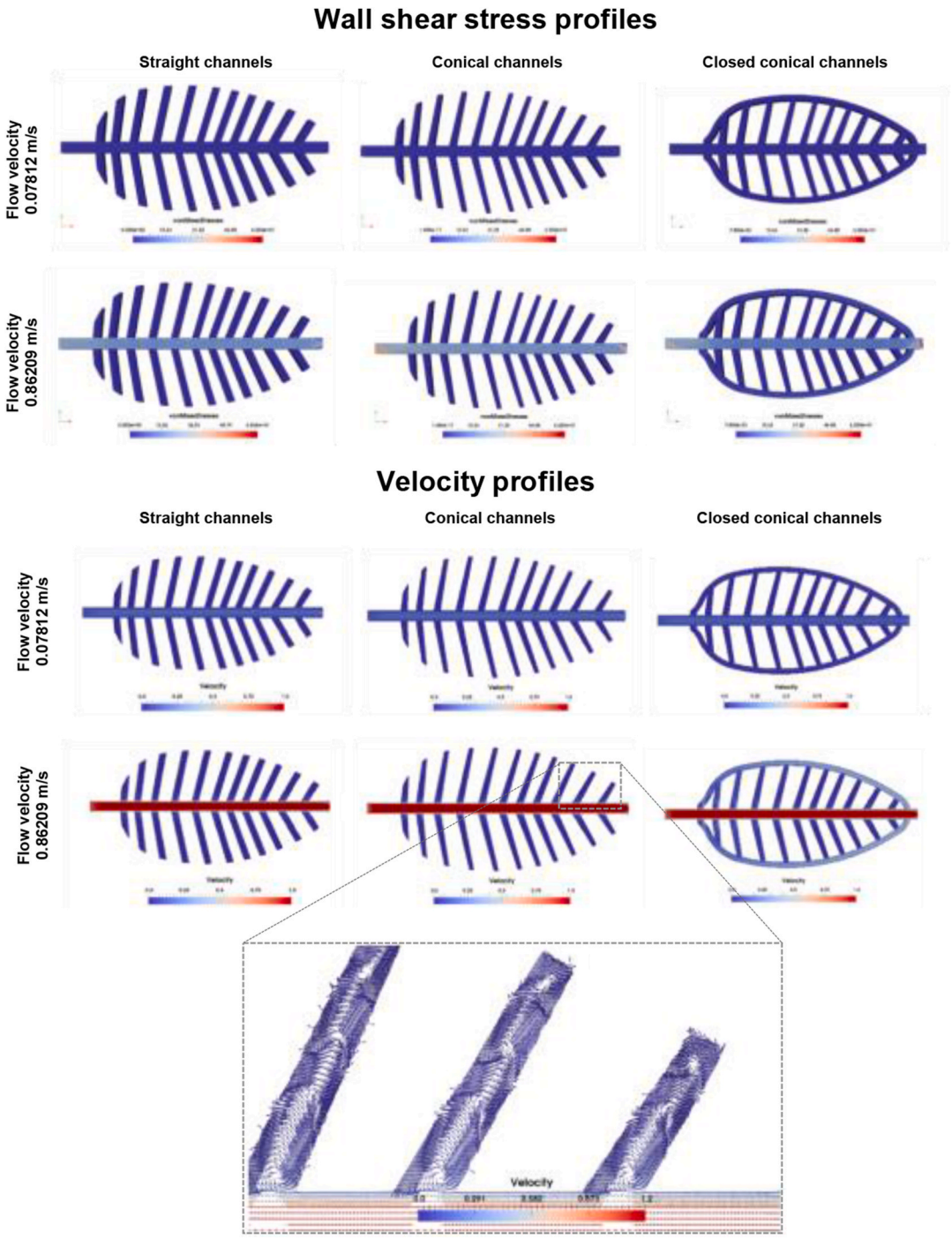

Fig. 8. Flow simulations using different leaf designs. Wall shear-stress profiles and velocity profiles investigated for the different designs at two different flow-velocity inputs (0.07812 m/s and 0.86209 m/s). There was a clear flow path inside the leaves and where the highest velocities were observed around the central channel, whereas the lateral channels showed slow velocities. Some recirculation and flow-separation areas were observed in parts of the lateral channels.

CRediT authorship contribution statement

Sanna Sämfors: Conceptualization, Methodology, Investigation, Writing – original draft, Writing – review & editing, writing – original draft preparation, reviewing and editing. **Essi M. Niemi:** Methodology, Investigation, Writing – original draft, Writing – review & editing. **Kristin Oskarsdotter:** Methodology, Investigation. **Claudia Villar Egea:** Methodology, Investigation. **Andreas Mark:** Methodology, Software, Writing – original draft, Writing – review & editing. **Hanne Scholz:** Conceptualization, Supervision, Writing – review & editing, Funding acquisition. **Paul Gatenholm:** Conceptualization, Supervision, Writing – review & editing, Funding acquisition.

Declaration of competing interest

The authors declare that they have no known competing financial interests or personal relationships that could have appeared to influence the work reported in this paper.

Acknowledgments

We would like to acknowledge Drs. Peter Apelgren and Lars Kölby

from Gothenburg University, Sahlgrenska Academy, Institute of Clinical Sciences, Department of Plastic Surgery, for providing the lipoaspirate. The Knut and Alice Wallenberg Foundation is gratefully acknowledged for sponsoring the Wallenberg Wood Science Center. This work was partly supported by the Research Council of Norway through its 3D TUNINK funding scheme (project no. 29675). Additionally, we would like to acknowledge the assistance in the *in vivo* experiment received from Merete Høyem at Oslo University Hospital. We would also like to acknowledge the help received from Jason Fye, M.S., Ph.D., with English language editing.

References

[1] E.C. Novosel, C. Kleinhans, P.J. Kluger, Vascularization is the key challenge in tissue engineering, Adv. Drug Deliv. Rev. 63 (4-5) (2011) 300–311.
[2] M. Lovett, K. Lee, A. Edwards, D.L. Kaplan, Vascularization strategies for tissue engineering, Tissue Eng. B Rev. 15 (3) (2009) 353–370.
[3] J.J. Kim, L. Hou, N.F. Huang, Vascularization of three-dimensional engineered tissues for regenerative medicine applications, Acta Biomater. 41 (2016) 17–26.
[4] P. Datta, B. Ayan, I.T. Ozbolat, Bioprinting for vascular and vascularized tissue biofabrication, Acta Biomater. 51 (2017) 1–20.
[5] S.V. Murphy, A. Atala, 3D bioprinting of tissues and organs, Nat. Biotechnol. 32 (8) (2014) 773–785.
[6] D. Kumar, A. Lyness, I. Gerges, C. Lenardi, N.R. Forsyth, Y. Liu, Stem cell delivery with polymer hydrogel for treatment of intervertebral disc degeneration: from 3D culture to design of the delivery device for minimally invasive therapy, Cell Transplant. 25 (12) (2016) 2213–2220.
[7] B.G. Ballios, M.J. Cooke, D. van der Kooy, M.S. Shoichet, A hydrogel-based stem cell delivery system to treat retinal degenerative diseases, Biomaterials 31 (9) (2010) 2555–2564.
[8] J.S. Choi, H.-J. Yang, B.S. Kim, J.D. Kim, J.Y. Kim, B. Yoo, K. Park, H.Y. Lee, Y. W. Cho, Human extracellular matrix (ECM) powders for injectable cell delivery and adipose tissue engineering, J. Contr. Release 139 (1) (2009) 2–7.
[9] S.J. Sullivan, T. Maki, K.M. Borland, M.D. Mahoney, B.A. Solomon, T.E. Muller, A. P. Monaco, W.L. Chick, Biohybrid artificial pancreas: long-term implantation studies in diabetic, pancreatectomized dogs, Science 252 (5006) (1991) 718–721.
[10] M. Brišŝová, I. Lacik, A. Powers, A. Anilkumar, T. Wang, Control and measurement of permeability for design of microcapsule cell delivery system, J. Biomed. Mater. Res.: Off. J. Soc. Biomater. Jpn. Soc. Biomater. Aus. Soc. Biomater. 39 (1) (1998) 61–70.
[11] S.H. Cartmell, B.D. Porter, A.J. García, R.E. Guldberg, Effects of medium perfusion rate on cell-seeded three-dimensional bone constructs in vitro, Tissue Eng. 9 (6) (2003) 1197–1203.
[12] S.N. Nazhat, E.A. Abou Neel, A. Kidane, I. Ahmed, C. Hope, M. Kershaw, P.D. Lee, E. Stride, N. Saffari, J.C. Knowles, Controlled microchannelling in dense collagen scaffolds by soluble phosphate glass fibers, Biomacromolecules 8 (2) (2007) 543–551.
[13] M. Radisic, H. Park, F. Chen, J.E. Salazar-Lazzaro, Y. Wang, R. Dennis, R. Langer, L. E. Freed, G. Vunjak-Novakovic, Biomimetic approach to cardiac tissue engineering: oxygen carriers and channeled scaffolds, Tissue Eng. 12 (8) (2006) 2077–2091.
[14] L. Yang, S.V. Shridhar, M. Gerwitz, P. Soman, An in vitro vascular chip using 3D printing-enabled hydrogel casting, Biofabrication 8 (3) (2016), 035015.
[15] J.S. Miller, K.R. Stevens, M.T. Yang, B.M. Baker, D.-H.T. Nguyen, D.M. Cohen, E. Toro, A.A. Chen, P.A. Galie, X. Yu, Rapid casting of patterned vascular networks for perfusable engineered three-dimensional tissues, Nat. Mater. 11 (9) (2012) 768–774.
[16] S. Sämfors, K. Karlsson, J. Sundberg, K. Markstedt, P. Gatenholm, Biofabrication of bacterial nanocellulose scaffolds with complex vascular structure, Biofabrication 11 (4) (2019), 045010.
[17] P.S. Gungor-Ozkerim, I. Inci, Y.S. Zhang, A. Khademhosseini, M.R. Dokmeci, Bioinks for 3D bioprinting: an overview, Biomater. Sci. 6 (5) (2018) 915–946.
[18] C. Mandrycky, Z. Wang, K. Kim, D.-H. Kim, 3D bioprinting for engineering complex tissues, Biotechnol. Adv. 34 (4) (2016) 422–434.
[19] N. Noor, A. Shapira, R. Edri, I. Gal, L. Wertheim, T. Dvir, 3D printing of personalized thick and perfusable cardiac patches and hearts, Adv. Sci. 6 (11) (2019) 1900344.
[20] P. Sasmal, P. Datta, Y. Wu, I.T. Ozbolat, 3D bioprinting for modelling vasculature, Microphysiol. Syst. 2 (2018).
[21] Y.S. Zhang, A. Arneri, S. Bersini, S.-R. Shin, K. Zhu, Z. Goli-Malekabadi, J. Aleman, C. Colosi, F. Busignani, V. Dell'Erba, Bioprinting 3D microfibrous scaffolds for engineering endothelialized myocardium and heart-on-a-chip, Biomaterials 110 (2016) 45–59.
[22] L. Ouyang, J.P. Armstrong, Q. Chen, Y. Lin, M.M. Stevens, Void-free 3D bioprinting for in situ endothelialization and microfluidic perfusion, Adv. Funct. Mater. 30 (1) (2020) 1908349.
[23] L. Dai, T. Cheng, C. Duan, W. Zhao, W. Zhang, X. Zou, J. Aspler, Y. Ni, 3D printing using plant-derived cellulose and its derivatives: a review, Carbohydr. Polym. 203 (2019) 71–86.
[24] G. Helenius, H. Bäckdahl, A. Bodin, U. Nannmark, P. Gatenholm, B. Risberg, In vivo biocompatibility of bacterial cellulose, J. Biomed. Mater. Res. Part A: An Official Journal of The Society for Biomaterials, The Japanese Society for Biomaterials, and The Australian Society for Biomaterials and the Korean Society for Biomaterials 76 (2) (2006) 431–438.
[25] K. Markstedt, A. Mantas, I. Tournier, H.c. Martínez Ávila, D. Hagg, P. Gatenholm, 3D bioprinting human chondrocytes with nanocellulose–alginate bioink for cartilage tissue engineering applications, Biomacromolecules 16 (5) (2015) 1489–1496.
[26] A. Bodin, L. Ahrenstedt, H. Fink, H. Brumer, B. Risberg, P. Gatenholm, Modification of nanocellulose with a xyloglucan–RGD conjugate enhances adhesion and proliferation of endothelial cells: implications for tissue engineering, Biomacromolecules 8 (12) (2007) 3697–3704.
[27] V.B.V. Tortorella S, M. Maturi, L. Sambri, M. Comes Franchini, E. Locatelli, Surface-modified nanocellulose for application in biomedical engineering and nanomedicine: a review, Int. J. Nanomed. 15 (2020) 9909–9937.
[28] J. Leppiniemi, P. Lahtinen, A. Paajanen, R. Mahlberg, S. Metsä-Kortelainen, T. Pinomaa, H. Pajari, I. Vikholm-Lundin, P. Pursula, V.P. Hytönen, 3D-printable bioactivated nanocellulose–alginate hydrogels, ACS Appl. Mater. Interfaces 9 (26) (2017) 21959–21970.
[29] N. Isobe, D.-S. Lee, Y.-J. Kwon, S. Kimura, S. Kuga, M. Wada, U.-J. Kim, Immobilization of protein on cellulose hydrogel, Cellulose 18 (5) (2011) 1251.
[30] K. Pietrucha, E. Marzec, M. Kudzin, Pore structure and dielectric behaviour of the 3D collagen-DAC scaffolds designed for nerve tissue repair, Int. J. Biol. Macromol. 92 (2016) 1298–1306.
[31] J. Di Russo, A.L. Luik, L. Yousif, S. Budny, H. Oberleithner, V. Hofschröer, J. Klingauf, E. van Bavel, E.N. Bakker, P. Hellstrand, Endothelial basement membrane laminin 511 is essential for shear stress response, EMBO J. 36 (2) (2017) 183–201.
[32] A. Pozzi, P.D. Yurchenco, R.V. Iozzo, The nature and biology of basement membranes, Matrix Biol. 57 (2017) 1–11.
[33] M. Marchand, C. Monnot, L. Muller, S. Germain, Extracellular Matrix Scaffolding in Angiogenesis and Capillary Homeostasis, Seminars in Cell & Developmental Biology, Elsevier, 2019, pp. 147–156.
[34] J. Song, X. Zhang, K. Buscher, Y. Wang, H. Wang, J. Di Russo, L. Li, S. Lütke-Enking, A. Zarbock, A. Stadtmann, Endothelial basement membrane laminin 511 contributes to endothelial junctional tightness and thereby inhibits leukocyte transmigration, Cell Rep. 18 (5) (2017) 1256–1269.
[35] F. Bianchi, M. Maioli, E. Leonardi, E. Olivi, G. Pasquinelli, S. Valente, A.J. Mendez, C. Ricordi, M. Raffaini, C. Tremolada, A new nonenzymatic method and device to obtain a fat tissue derivative highly enriched in pericyte-like elements by mild mechanical forces from human lipoaspirates, Cell Transplant. 22 (11) (2013) 2063–2077.
[36] C. Tremolada, V. Colombo, C. Ventura, Adipose tissue and mesenchymal stem cells: state of the art and Lipogems® technology development, Curr. Stem Cell Rep. 2 (3) (2016) 304–312.
[37] S. Schive, R. Fjukstad, D. Josefsen, M. Katavic, S. Abadpour, H. Gullestad, G. Kvalheim, H. Scholz, Automated Isolation and Expansion of Human Adipose Tissue-Derived Stem Cells for a Seamless Translation into Clinical Trials.
[38] A. Mark, R. Rundqvist, F. Edelvik, Comparison between different immersed boundary conditions for simulation of complex fluid flows, Fluid Dynam. Mater. Process. 7 (3) (2011) 241–258.
[39] A. Mark, B.G. van Wachem, Derivation and validation of a novel implicit second-order accurate immersed boundary method, J. Comput. Phys. 227 (13) (2008) 6660–6680.
[40] J. Ahrens, B. Geveci, C. Law, Paraview: an end-user tool for large data visualization, in: The visualization handbook, 2005, p. 717.
[41] M. Klarhöfer, B. Csapo, C. Balassy, J. Szeles, E. Moser, High-resolution blood flow velocity measurements in the human finger, Magn. Reson. Med.: Off. J. Int. Soc. Magn. Resonance Med. 45 (4) (2001) 716–719.
[42] K. Säljö, L.S. Orrhult, P. Apelgren, K. Markstedt, L. Kölby, P. Gatenholm, Successful engraftment, vascularization, and in vivo survival of 3D-bioprinted human lipoaspirate-derived adipose tissue, Bioprinting 17 (2020), e00065.
[43] N.Y. Lin, K.A. Homan, S.S. Robinson, D.B. Kolesky, N. Duarte, A. Moisan, J. A. Lewis, Renal reabsorption in 3D vascularized proximal tubule models, Proc. Natl. Acad. Sci. Unit. States Am. 116 (12) (2019) 5399–5404.
[44] C. Mandrycky, B. Hadland, Y. Zheng, 3D curvature-instructed endothelial flow response and tissue vascularization, Sci. Adv. 6 (38) (2020), eabb3629.
[45] A. Hartsock, W.J. Nelson, Adherens and tight junctions: structure, function and connections to the actin cytoskeleton, Biochim. Biophys. Acta Biomembr. 1778 (3) (2008) 660–669.
[46] J.R. Privratsky, P.J. Newman, PECAM-1: regulator of endothelial junctional integrity, Cell Tissue Res. 355 (3) (2014) 607–619.
[47] D. Vestweber, VE-cadherin: the major endothelial adhesion molecule controlling cellular junctions and blood vessel formation, Arterioscler. Thromb. Vasc. Biol. 28 (2) (2008) 223–232.
[48] A. Rabodzey, Y. Yao, F.W. Luscinskas, S.K. Shaw, C.F. Dewey Jr., Early response of endothelial cells to flow is mediated by VE-cadherin, Cell Commun. Adhes. 14 (5) (2007) 195–209.
[49] A.M. Müller, M.I. Hermanns, C. Skrzynski, M. Nesslinger, K.-M. Müller, C. J. Kirkpatrick, Expression of the endothelial markers PECAM-1, vWf, and CD34 in vivo and in vitro, Exp. Mol. Pathol. 72 (3) (2002) 221–229.